



Original Article

Anti-inflammatory Role of Euphorbiasteroid in Rheumatoid Arthritis



Huancai Fan¹, Ruojia Zhang¹, Shufeng Li², Haojun Shi³, Yi Li⁴, Yun Geng⁵, Yuang Zhang¹, Dandan Shi¹, Ting Wang¹, Xifeng Li¹, Tingting Zhang¹, Jihong Pan^{1,6}, Luna Ge^{1,6} and Guanhua Song^{7*}

¹Biomedical Sciences College & Shandong Medicinal Biotechnology Centre, Key Lab for Biotech-Drugs of National Health Commission, Key Lab for Rare & Uncommon Diseases of Shandong Province, Shandong First Medical University & Shandong Academy of Medical Sciences, Jinan, China; ²Department of Orthopedic Surgery, The First Affiliated Hospital of Shandong First Medical University, Jinan, China; ³The second clinical medical college, Henan University of Chinese Medicine, Zhengzhou, China; ⁴Department of Joint Surgery, Shandong Provincial Hospital Affiliated to Shandong University, Jinan, China; ⁵Shandong First Medical University & Shandong Academy of Medical Sciences, Jinan, China; ⁶Department of Rheumatology and Autoimmunology, The First Affiliated Hospital of Shandong First Medical University, Jinan, China; ⁷Institute of Basic Medicine, Shandong First Medical University & Shandong Academy of Medical Sciences, Jinan, China

Received: December 12, 2021 | Revised: February 15, 2022 | Accepted: February 22, 2022 | Published: April 01, 2022

Abstract

Background and objectives: Euphorbiasteroid (EUP) is one of the ingredients of traditional Chinese medicinal plants with anti-inflammatory activity. This study aimed to evaluate the effect of EUP in rheumatoid arthritis (RA).

Materials and methods: Cell Counting Kit-8 (CCK8) and 5-Ethynyl-2'-deoxyuridine (EdU) were performed to detect the proliferation of fibroblast-like synoviocytes (FLSs). The expression of cytokines was detected by quantitative real-time polymerase chain reaction (RT-qPCR) and enzyme-linked immunosorbent assay (ELISA). The Transwell system without the gel was utilized to detect the cell migration. The pro-angiogenesis ability of HUVECs was detected by tube formation assay. EUP was introduced into the collagen-induced arthritis (CIA) model to determine its therapeutic effect, as measured by microcomputed tomography (micro-ct) and hematoxylin-eosin (H&E) staining. AKT1 was enriched by network pharmacology and molecular docking techniques. Western blot, immunofluorescence (IF) and RT-qPCR were conducted to detect the effects of EUP on AKT1.

Results: When RA FLSs were treated with EUP, the proliferation of RA FLSs decreased in a dose- and time-dependent manner. Furthermore, the production of inflammatory cytokines, cell migration and proangiogenic ability of RA FLSs were suppressed by the EUP treatment. The in vivo experiments revealed that EUP can significantly reduce the severity of the CIA model by decreasing the paw thickness, arthritis score, cartilage degeneration, joint destruction, and serum inflammatory cytokine level. The network pharmacology and molecular docking predicted AKT1 as the target, in which EUP exerts its effects. The western blot, IF and RT-qPCR identified the toll-like receptor signaling pathway and its key component, AKT1, as potential targets, in which EUP exerts its anti-arthritis effects in RA.

Keywords: Rheumatoid arthritis; Euphorbiasteroid; Fibroblast-like synoviocytes; Toll-like receptor signaling pathway; AKT1.

Abbreviations: CIA, collagen-induced arthritis; EUP, Euphorbiasteroid; FLS, fibroblast-like synoviocytes; IL, interleukin; RA, rheumatoid arthritis; TCM, Traditional Chinese medicine; TNF, tumor necrosis factor.

*Correspondence to: Guanhua Song, Institute of Basic Medicine, Shandong First Medical University & Shandong Academy of Medical Sciences, Qingdao Road, Jinan 250017, China. ORCID: <https://orcid.org/0000-0002-1359-515X>. Tel: +86-531-59567360, Fax: +86-531-59567355, E-mail: yysghy@163.com

How to cite this article: Fan H, Zhang R, Li S, Shi H, Li Y, Geng Y, et al. Anti-inflammatory Role of Euphorbiasteroid in Rheumatoid Arthritis. *Explor Res Hypothesis Med* 2022;7(4):217–227. doi: 10.14218/ERHM.2021.00076.

Conclusions: EUP ameliorates the deterioration of RA by inactivating the toll-like receptor signaling pathway via AKT1. Therefore, EUP might hold potential as a treatment medicine for RA.

Table 1. The list of all primers used in the study

Gene name	Sense (5'-3')	Antisense (5'-3')
GAPDH (homo)	GCA CCG TCA AGG CTG AGA AC	TGG TGA AGA CGC CAG TGG A
IL-8 (homo)	ATCA CAG GTA GTG AGA CCG A	AGC TGA TGT GAA GTA GTT CTT AG
IL-β (homo)	ATG ATG GCT TAT TAC AGT GGC A	GTC GGA GAT TCG TAG CTG GA
IL-6 (homo)	ACT CAC CTC TTC AGA ACG AAT TG	CCA TCT TTG GAA GGT TCA GGT TG
MMP3 (homo)	CTG GAC TCC GAC ACT CTG GA	CAG GAA AGG TTC TGA AGT GAC C
CCL2 (homo)	CAG CCA GAT GCA ATC AAT GCC	TGG AAT CCT GAA CCC ACT TCT
TNF-α (homo)	TGT GAG GAG GAC GAA CAT C	GTG GTC TTG TTG CTT AAA GTT CTA

Introduction

Rheumatoid arthritis (RA) is a common systemic inflammatory autoimmune disease characterized by painful, swollen joints that can severely impair physical function and quality of life.¹ Inflammation starts in the synovium of the joints, leading to the destruction of cartilage, bone and other adjacent tissues, and the formation of pannus. The main reason is that T cells, B cells, macrophages, dendritic cells (DCs) and synovial cells are induced by their antigens to participate in the immune response, and release inflammatory cytokines that mediate cartilage erosion and joint injury.² In recent years, the use of disease-improving anti-rheumatic drugs (DMARDs) has been proven to be effective for disease management.³ However, long-term treatment with DMARDs is often poorly tolerated, and some patients do not respond well to existing treatments, leading to the continuous destruction of joints.⁴ Therefore, identifying novel treatment strategies for RA remains as the main focus in this field. In the active stage of RA, pro-inflammatory factors occupy a dominant position. Rebuilding the balance between pro-inflammatory factors and anti-inflammatory factors has become an important treatment goal in RA.

Traditional Chinese medicine (TCM) has a long history of preventing the progression of RA, and the monomers of Chinese medicine are effective ingredients in Chinese herbal medicine. Furthermore, the oral administration of these monomers is characterized by low antigenicity, but high safety and patient compliance, small molecular weights, and relatively stable properties.⁵ EUP is a tricyclic diterpene found in sesame seeds, which is one of the TCM plants. This can inhibit the activity of tyrosinase, enhance the phosphorylation of AMPK, and has a variety of biological activities, such as anticancer, antiviral, and multidrug resistance regulation activities.^{6,7} The present study aimed to determine the therapeutic effects and mechanism of EUP in RA, and reveal its potential in the treatment of RA.

Materials and methods

Subjects

Synovial tissues were taken from patients (four females and six males) undergoing joint replacement in Qianfoshan Hospital (The First Affiliated Hospital of Shandong First Medical University, Shandong, China). All 10 patients met the 1987 American College of Rheumatology revised RA diagnostic criteria, and all patients were informed and agreed to participate in the study. The present study conformed to the ethics guidelines of the Declaration of Helsinki. All appropriate measures were taken to minimize the pain or

discomfort of animals. This study was carried out in accordance with the recommendations in the Guide for the Care and Use of Laboratory Animals of the Institutional Animal Care and Use Committee of Shandong First Medical University & Shandong Academy of Medical Sciences and the study protocol was approved by the Institutional Review Board of Shandong Medicinal Bio-technology Center (VCMC08BR067). Furthermore, the manuscript was prepared according to the Animal Research: Reporting of In Vivo Experiments (ARRIVE) guidelines (Supplementary File 1).

Cell culture, isolation and stimulation

Synovial tissues were treated by collagenase II and III (Solarbio, China) for the digestion and extraction for RA fibroblast-like synoviocytes (FLSs). Then, these were cultured in Dulbecco's modified Eagle's medium (DMEM) supplemented with 1% penicillin-streptomycin antibiotic and 15% fetal bovine serum (FBS).

Next, the cells were sub-cultured for 4–6 generations, and seeded in a 24-well plate ($3-5 \times 10^5$ cells/well). After starvation treatment for 16 hours to avoid the effects of serum on the experiment, EUP (20 μM and 50 μM) was added. After incubation for approximately six hours, interleukin (IL) 1β (IL1β, 10 ng/mL; Solarbio, China) and tumor necrosis factor-α (TNF-α, 10 ng/mL; Solarbio, China), or lipopolysaccharide (LPS, 10 μg/mL; Solarbio, China) were added for another 20 hours.

RT-qPCR

RNA was extracted by Trizol (Vazyme, China). The RT-qPCR procedure was performed in the Light-Cycler 480 System (Basel Roche, Switzerland), in order to detect the expression levels of IL6, IL8, matrix metalloproteinase-3 (MMP3), and C-C motif chemokine ligand 2 (CCL2). All primers (BGI, China) are presented in Table 1. Then, all results were calculated using the comparative cycle threshold method ($2^{-\Delta\Delta CT}$), and the graph was drawn using Graph Prism 7.04.

Cell viability

Cell viability assays were conducted, as previously described.⁸ Briefly, 2×10^3 RA FLSs were inoculated in a 96-well plate. When the cells grew to a suitable density, EUP was added at different concentrations (20 μM and 50 μM) for 24 hours. Then, CCK-8 (10 μL) was added, and the RA FLSs were cultured at 37°C in a 5% CO₂ incubator for one hour. Afterwards, 450 nm of wavelength was measured on a microplate reader.

CCK-8 proliferation assay

After RA FLSs were inoculated in a 96-well plate, EUP (20 μ M and 50 μ M) was added for 24, 48 and 72 hours. The experiment was performed according to the instructions of the reagent manufacturer (Sigma-Aldrich): 10 μ L of CCK-8 reagent was added, and these were cultured at 37°C in a 5% CO₂ incubator for one hour. The determination method was described above as cell viability.

EdU proliferation assay

The EdU proliferation assay was conducted, as previously described.⁹ A total of 1×10^4 cells were inoculated in a 24-well plate. Then, EUP (20 μ M and 50 μ M) was added for 48 hours, and cultured in an incubator. This experiment was performed according to the instructions of the reagent manufacturer (Ribobio, Guangzhou, China). Five fields were randomly selected for counting and analysis.

Migration and tube formation assay

The migration assay (Transwell) was performed, as previously described.¹⁰ FLSs were added with EUP (20 μ M and 50 μ M) for 24 hours. Then, the RA FLSs were trypsinized and inoculated in a 24-well plate chamber (1% penicillin-streptomycin antibiotic and 15% FBS). After adherence to the wall, the medium in the upper chamber was replaced (1% penicillin-streptomycin antibiotic and 2% FBS, at a total volume of 200 μ L). Then, phosphate buffer saline (PBS) was used to wash the cells after 10 hours. Afterwards, 4% paraformaldehyde was used to fix the RA FLSs for 40 minutes, staining was performed with crystal violet for 40 minutes, and these were washed again with PBS. Subsequently, these were observed in five randomly chosen fields. The angiogenesis ability of human umbilical vein endothelial cells (HUVECs) after EUP (20 μ M and 50 μ M) treatment was determined by tube formation. The Matrigel was initially pre-coated in a 48-well culture plate, and dried in an incubator at 37°C for 50 minutes. Then, the HUVECs (5×10^5 cells/mL) were treated with EUP for 24 hours after stimulation with TNF- α and IL1 β . Afterwards, these were trypsinized, resuspended, and seeded to the 48-well plate that contained the Matrigel. Subsequently, the capillary tube formation of each well in the culture plate was photographed in five randomly chosen fields. The experiments were conducted in triplicate.

The CIA model

Twelve male DBA mice (approximately eight weeks old; Vital River Laboratory Animal Technology, China) were induced into the CIA model, as previously described.¹¹ The DBA mice were induced with bovine type II collagen (2 mg/mL, Chondrex, $n = 6$ mice per group) through intradermal injection at the base of the tail, twice. The first injection was equally mixed with Freund's complete adjuvant (Sigma-Aldrich). After 21 days, a second injection, which was equally mixed with Freund's incomplete adjuvant (Sigma-Aldrich), was administered. After two weeks, the hind paw thickness and arthritis score were evaluated every three days. According to the scores, mice were randomly divided into two groups. The scoring standard was determined, as previously described.¹² The CIA models were injected with the same amount of EUP, while mice that received an equal amount of dimethyl

sulfoxide (DMSO) served as the vehicle control (DMSO group). Mice in the control group did not receive collagen induction. All appropriate measures were taken to minimize the pain or discomfort of the animals. The present study was approved by the Medical Ethics Committee of the Institutional Review Board of Shandong Medicinal Biotechnology Center (SMBC2020-07), and the Institutional Animal Care Committee for the Husbandry, Care and Experimentation of Animals.

Microcomputed tomography (micro-ct) scanning

Micro-ct (QuantumGX, USA) was used to scan elbows, knees, front and back paws of mice. Scanning parameters: x-ray kV: 90 kV; x-ray uA: 88 uA; scan time: 14 minutes; FOV: 18 mm; pixel size: 36.0 μ m; 512 slices were selected to determine the bone microarchitecture. The tibia trabecular analysis included the relative volume of the trabecular bone (BV/TV, %), the trabecular bone density (Tb.BMD, g/cm³), the trabecular bone thickness (Tb.Th, mm), and the trabecular bone separation (Tb.Sp, mm).

Hematoxylin-eosin (H&E) staining

The elbows and knee joints of mice were fixed using tissue fixative solution for 18 hours, and decalcified by 10% EDTA for another 28 days. During this period, 10% of the EDTA was replaced every three days. Then, the samples were submerged in paraffin, sectioned, and stained with the H&E reagent.

Enzyme-linked immunosorbent assay (ELISA)

Cells were cultured and stimulated, as described above.¹² Then, the supernatant was collected and diluted at a certain proportion (1:4). Afterwards, the diluted antibody was added to the 96-well plate, centrifuged at 300 rpm/min, and incubated at room temperature for 1.5 hours. Then, the plate was washed, enzyme was added for incubation, the substrate for color development was added, cells were terminated, the dual wavelength was detected and analyzed, and the expression of IL6, IL8 and MCP1 in the supernatant of RA FLSs was measured, according to manufacturer instructions (R&D Systems, USA).

Target prediction

The PubChem database was used to determine the EUP chemical structure, SMILES file, molecular weight and PubChem CID, and predict the target of EUP through TCMSP, STITCH, Swiss Target-Prediction, and other databases. Through the GeneCards (www.genecards.org/), NCBI-Gene (www.ncbi.nlm.nih.gov/gene), DrugBank (www.drugbank.ca/) and OMIM (www.omim.org/) databases, the inflammation-related targets were identified, with RA as the keyword, and all targets were summarized according to gene name. Then, the predicted effects of EUP and rheumatoid-related targets were compared. The intersection was determined using a Venn diagram, and KEGG analysis was performed for these targets.

Immunofluorescence (IF)

Cells were seeded in a 48-well plate, and RA FLSs were treated with EUP (20 μ M) for 24 hours, as described above. Then, these

were incubated with AKT1 (ab182928, 1:1,000; Abcam, Cambridge, MA, USA) overnight. Afterwards, these were incubated with the secondary antibody (1:10,000; ZSJB Co., Ltd., China), and stained with DAPI (249167, Sigma-Aldrich). Subsequently, these cells were observed by laser confocal microscopy, and photographed.

Western blot

RA FLSs were treated and collected in ice-cold lysis buffer, as previously described.¹² The program for the western blot was set at 80 V (20 minutes) and 120 V (60 minutes), and polyvinylidene fluoride (PVDF) membranes (IPFL00010; Merck, China) were used to transfer the proteins. Next, AKT1, P-AKT1 and GAPDH were incubated for 12–24 hours at room temperature. Then, the HRP-conjugated goat anti-rabbit IgG (Proteintech, China) was incubated for 80 minutes at 20°C. AKT1 (ab182928, 1:1,000), b182921 (ab278559) and GAPDH (ab8245) were purchased from Abcam (Cambridge, USA).

Small interfering RNA transfection

RA FLSs were treated with pro-inflammatory factors, as described above. After the RA FLSs grew to 70% confluence, the cells were transiently transfected with the siRNA of AKT1 and vehicle control (normal controls). The detailed procedures were performed, as previously described¹³ (siAKT1: sense, 5'-GGA GGG UUG GCU GCA CAA ATT-3'; anti-sense, 5'-UUU GUG CAG CCA ACC CUC CTT-3').

Statistics

The data were presented as mean \pm standard deviation (SD). Since the scores for arthritis and paw swelling did not meet the requirements for homogeneity of variance, Mann–Whitney U-test was used. The other results were assessed by analysis of variance (one-way ANOVA), followed by Tukey's honest significant difference test. A *p*-value of <0.05 was considered statistically significant.

Results

EUP reduced the proliferation of RA FLSs

The chemical structure of EUP is presented in Figure 1a. In order to determine the effects of EUP on RA FLSs, the cytotoxicity was initially analyzed. The cell viability results of the CCK-8 assay revealed that EUP does not affect cell growth at 0–10 μ M, when compared to the DMSO group. However, EUP treatment at 20–100 μ M can significantly reduce the viability of FLSs (Fig. 1b) in a time- and dose-dependent manner with the simultaneous stimulation of IL1 β and TNF- α . Therefore, EUP at concentrations of 20 μ M and 50 μ M were selected for the subsequent experiments. The detailed analysis results for the cell proliferation analyzed by CCK-8 assay revealed that cell proliferation decreases in a dose- and time-dependent manner, when RA FLSs are activated by IL1 β and TNF- α , and are exposed to EUP (20 μ M and 50 μ M) (Fig. 1c). Furthermore, the inhibitory effect of EUP was also duplicated by the EdU assay (Fig. 1d).

EUP treatment ameliorates the arthritis phenotype of RA FLSs

In order to determine whether EUP plays a role in anti-RA, the effect of EUP on the inflammatory phenotype of RA FLSs was analyzed. The stimulation with TNF- α and IL1 β significantly induced the expression of inflammatory cytokines, including IL6 (Fig. 2a), IL8 (Fig. 2b), CCL2 (Fig. 2c) and MMP3 (Fig. 2d), at the mRNA level. However, this induction was attenuated by the EUP treatment (Fig. 2a–d). The supernatant of the RA FLSs was collected and diluted at a ratio of 1:4 for the subsequent inflammatory cytokine (IL1 β and IL8) assays. Similar effects were also found in the ELISA results, in which the secretion of IL1 β (Fig. 2e) and IL8 (Fig. 2f) in the supernatant of RA FLSs was analyzed.

In addition, since extensive synovial hyperplasia and aggressive inflammation are the physiological characteristics of RA,¹² the migration of RA FLSs was detected. The results revealed that the migration ability of RA FLSs significantly increased upon activation of the stimulation of TNF- α and IL1 β (10 ng/mL) (Fig. 2g–h). However, this increase almost disappeared when RA FLSs were treated with EUP (20 μ M and 50 μ M).

Furthermore, the angiogenic ability of HUVECs, with or without EUP treatment, was determined by tube formation assay. The results revealed that EUP can inhibit the number of tube formations in HUVECs (Fig. 2i), when compared to those from parental control cells.

Effect of EUP on the collagen-induced CIA model

Next, the therapeutic effect of EUP (10 mg/kg) in the CIA model was detected. The paw thickness and swelling of arthritis were scored every three days. Compared to the DMSO group, the paw thickness decreased in the CIA model (Fig. 3a–b), and the swelling of arthritis (Fig. 3c) was significantly alleviated after EUP treatment. In order to assess the therapeutic potential of EUP, micro-CT was performed to quantify the bone destruction of the distal tibia and paws through a three-dimensional (3D) microstructure. It was found that BV/TV, Tb.Th and Tb.BMD significantly decreased, while Tb.Sp increased in the DMSO group. However, this induction was attenuated by the EUP treatment (Fig. 3d–g). Furthermore, compared to the DMSO group, the results in the 3D figures revealed that the degree of bone destruction was attenuated. Furthermore, the H&E staining also revealed that the degree of synovial hyperplasia and cartilage degeneration decreased in the EUP treatment group (Fig. 3h–i).

Mice serum was collected and diluted at a ratio of 1:2 for the subsequent cytokine (IL1 β , TNF- α and CCL2) assays. The results revealed that the expression levels of IL1 β (Fig. 3j), TNF- α (Fig. 3k) and CCL2 (Fig. 3l) significantly decreased in the EUP treatment group, when compared to the DMSO group. These results further support the notion that EUP treatment can reduce the level of chemokines. Furthermore, the inflammatory cytokines in mice ameliorated the physiological and biochemical characteristics.

Identifying the target genes of EUP

Online tools were used to predict the potential targets of EUP. A total of 21 potential targets of EUP were identified to be associated with RA by network pharmacologic analysis (Fig. 4a). According to the KEGG analysis, these potential targets mainly affect the

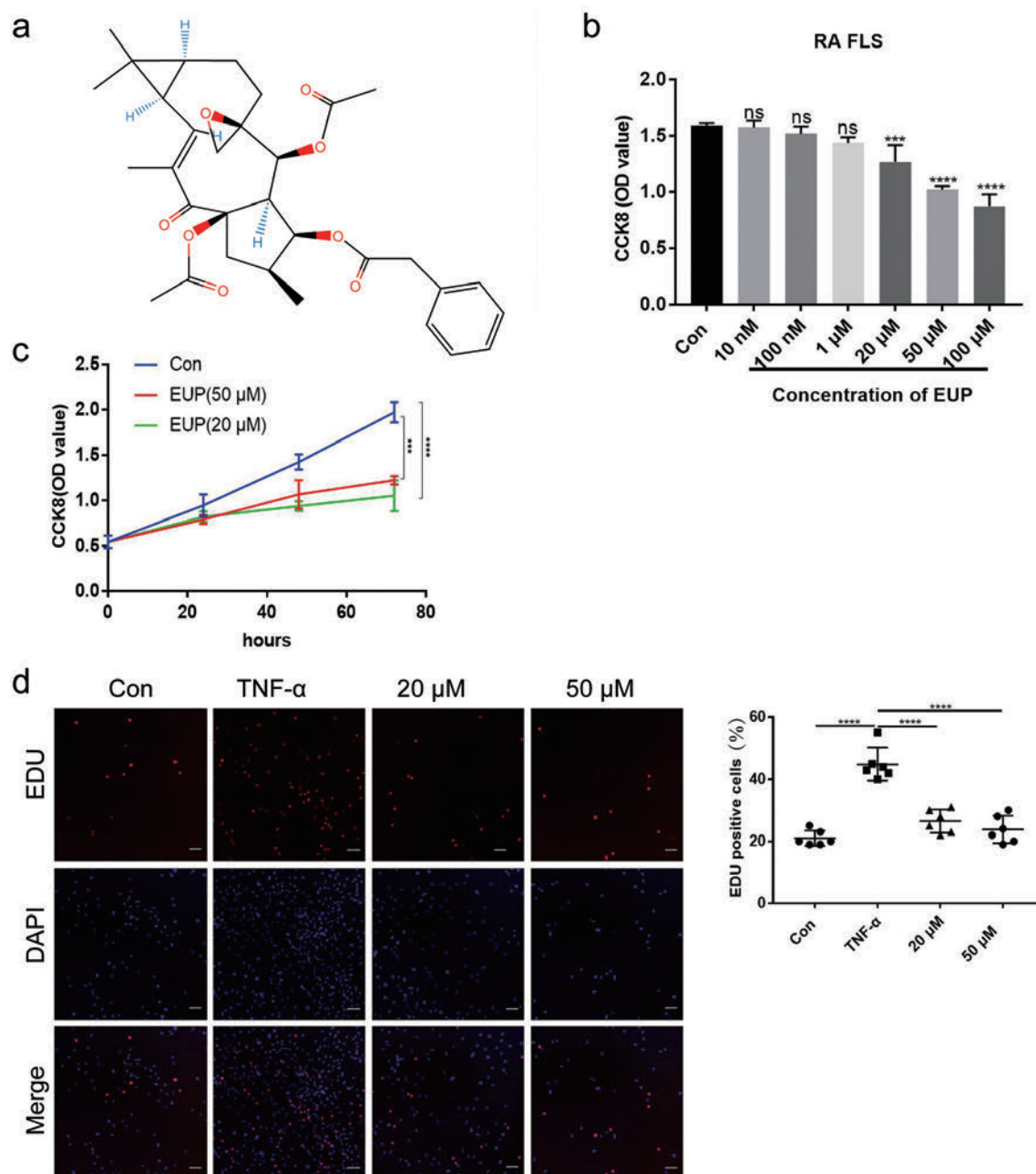


Fig. 1. EUP reduced the proliferation of RA FLSs. (a) The chemical structure of EUP. (b) The cytotoxicity analysis using CCK-8 in RA FLSs treated with different concentrations of EUP. (c) Cell proliferation using the CCK-8 proliferation assay in RA FLSs treated with EUP (20 μM and 50 μM). (d) Cell proliferation using EdU proliferation assay in RA FLSs treated with 20 μM and 50 μM of EUP (100×). The results were analyzed by one-way ANOVA, followed by Tukey's honest significant difference test. ns: non-significant, * $p < 0.05$, ** $p < 0.01$, vs. the indicated control group.

signaling pathways in measles, toxoplasmosis, osteoclast differentiation, apoptosis, and hepatitis B and C, the prolactin signaling pathway, the toll-like receptor signaling pathway, and folate biosynthesis (Fig. 4b). The STRING analysis revealed that AKT1 was at the key node (Fig. 4c). Through molecular docking technology, it was identified that EUP interacts with the THR160, THR312 and LYS276 of AKT1 (PDB: 4gv1) via hydrogen bonds (Fig. 4d), and PHE161, PHE442, LEU298 and GIU278 via hydrophobic interaction. Among these, GLU278 is commonly used as the binding site

of AKT1 inhibitors.^{14,15} All these data shows that AKT1 may play a major role in inhibiting EUP in the toll-like receptor signaling pathway.

EUP inactivates the toll-like receptor signaling pathway via AKT1

In the KEGG prediction and molecular docking analysis, focus

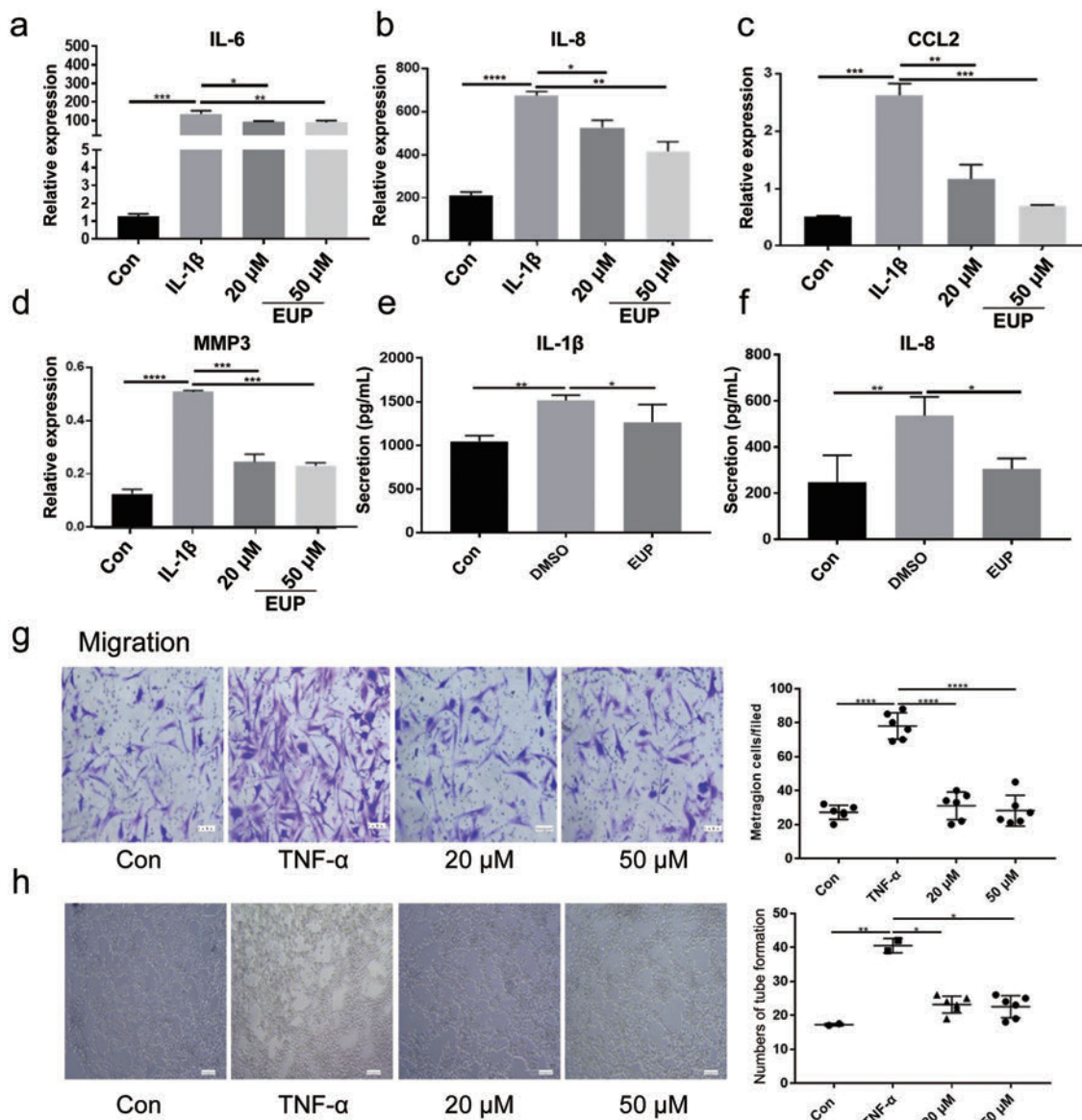


Fig. 2. EUP treatment ameliorates the arthritis phenotype of RA FLSS. (a–d) After exposure to the stimulation of inflammatory factors (the concentration used for IL1β and TNF-α was 10 ng/mL ETC) for six hours, RA FLSS were treated with EUP. The expression of IL6, IL8, CCL2 and MMP3, at the mRNA level, was measured by RT-qPCR. (e–f) The ELISA results in the supernatant of FLSS. (g) RA FLSS were collected, and the Transwell apparatus was used to measure the cell migration (100×). (h) The tube formation assay (100×) results revealed the angiogenic ability of HUVECs, with or without EUP treatment. The levels of the inflammatory factors were statistically analyzed by Tukey's test, vs. the indicated control group. * $p < 0.05$, ** $p < 0.01$, each experiment was performed in triplicate.

was given on the toll-like receptor signaling pathway and its target protein, AKT1.

The activation of the toll-like receptor signaling pathway in response to LPS activation was initially detected. The results revealed that LPS increased the expression of IL1β, TNF-α and IL6, which play an important role in the toll-like receptor signaling pathway. However, this induction was attenuated by the EUP treatment on RA FLSS (Fig. 5a–c).

Next, the intracellular expression of AKT1 was detected. Compared to the DMSO group, less AKT1 protein entered the nucleus after EUP treatment, in response to IL1β and TNF-α (10 ng/mL) (Fig. 5d). The western blot results revealed that the phosphoryl-

ated level of AKT1 (Ser473) increased after the activation IL1β and TNF-α. However, this induction was apparently attenuated by the EUP treatment (20 μM and 50 μM). The total AKT1 protein expression level was not affected by the challenge of EUP (Fig. 5e). In order to further confirm the correlation between the anti-RA effect of EUP and the toll-like receptor signaling pathway via AKT1, AKT1 was further silenced. Through stimulation, the RT-qPCR results revealed that the levels of IL1β, TNF-α, IL6, IL8, MMP3 and CCL2 (Fig. 5f–k) decreased after EUP treatment or AKT1 knockdown. However, no additional decrease was observed after the cells were treated with EUP and AKT1 knockdown (Fig. 5g–k), except for IL6 (Fig. 5f). These results prove that EUP can

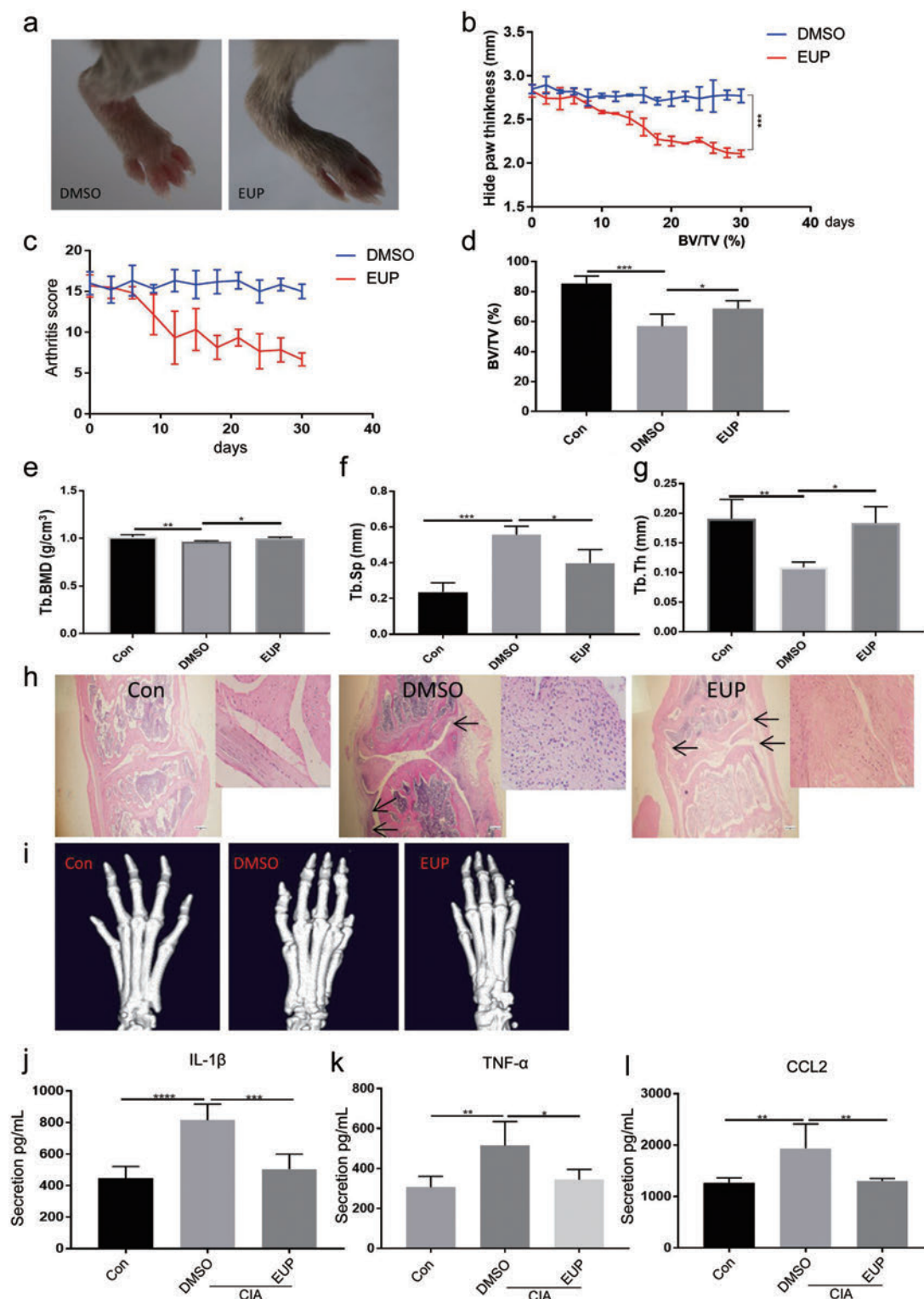


Fig. 3. Effect of EUP in the collagen-induced CIA animal models. (a) Photographs of the representative hind legs in the CIA model group, with or without EUP treatment. (b–c) The hind paw thickness and arthritis score were evaluated every three days, and the Mann-Whitney U-test was used. (d–g) The BV/TV, Tb.BMD, Tb.Sp and Tb.Th in the distal tibia were assayed by micro-ct. (h) Representative images of the H&E staining of the interphalangeal joint from the con, DMSO and EUP treatment groups. The changes in pathology (as indicated by the black arrows) are shown (40 \times). (i) The 3D images of mice paws, showing the joint swelling. (j–l) The levels of IL1 β , TNF- α and MCP1 in serum were determined by ELISA. The results were analyzed by one-way ANOVA, followed by Tukey's honest significant difference test. * $p < 0.05$, ** $p < 0.01$, vs. the indicated control group.

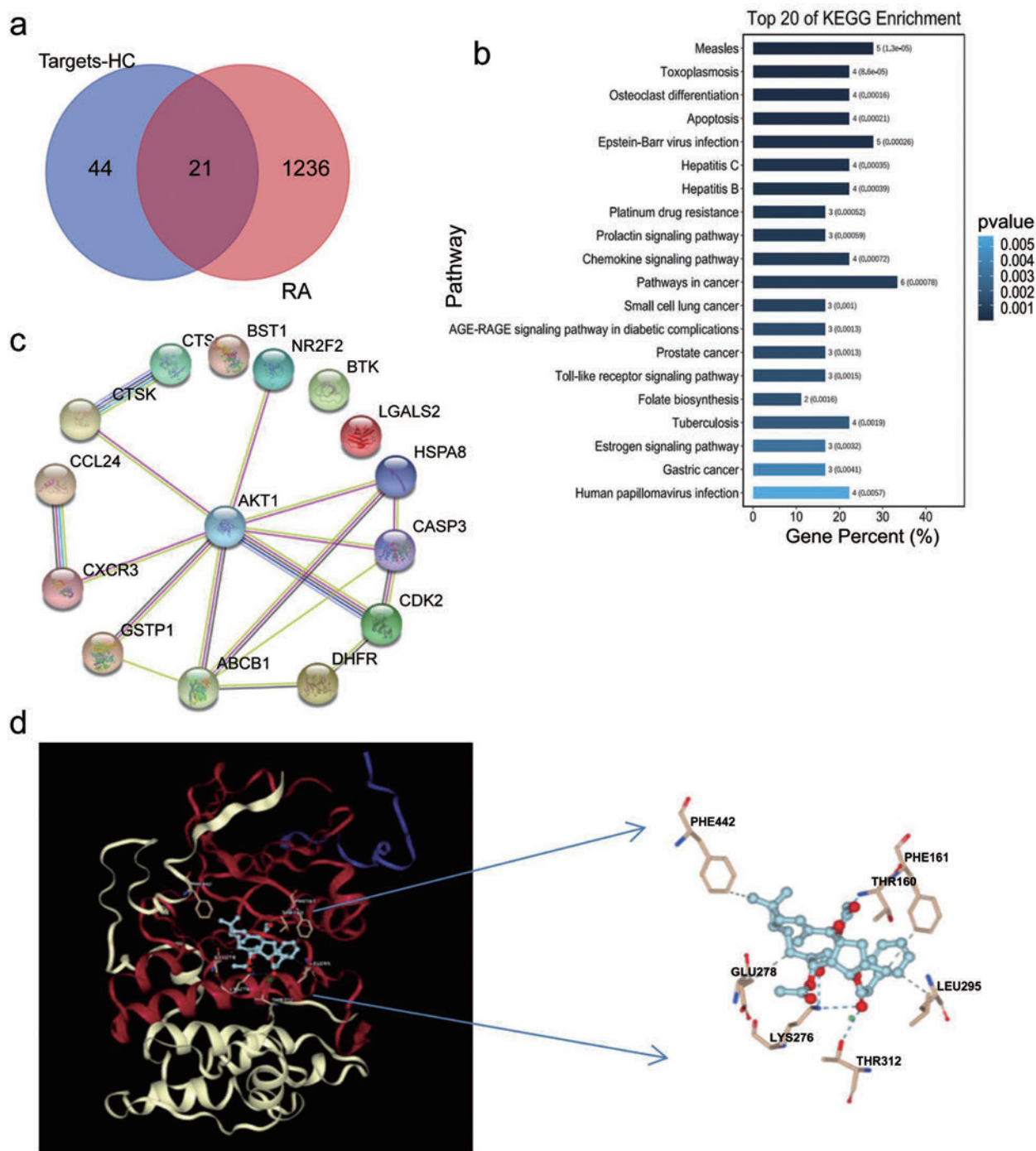


Fig. 4. Screening of the target genes of EUP. (a) The overlapping targets of RA and EUP. (b) The KEGG analysis presents the signaling pathways. (c) The STRING analysis revealed that AKT1 is the key node. (d) The molecular docking analysis of EUP shows its binding to the predicted target proteins (PDB: 4gv1).

slow down the occurrence and development of RA via the AKT1-mediated toll-like receptor signaling pathway.

Discussion

RA is characterized by persistent synovitis with excessive pro-

duction and expression of TNF- α , and excessive release of pro-inflammatory cytokines. FLSs abnormally proliferate, invade the cartilage, and cause joint destruction.^{16,17} RA treatment ranges from the use of nonsteroidal anti-inflammatory drugs (NSAIDs) and DMADs to biological agents (such as TNF- α inhibitors),¹⁸ glucocorticoids and corresponding surgical measures, but none of these can completely treat RA. Due to the dilemma of effective

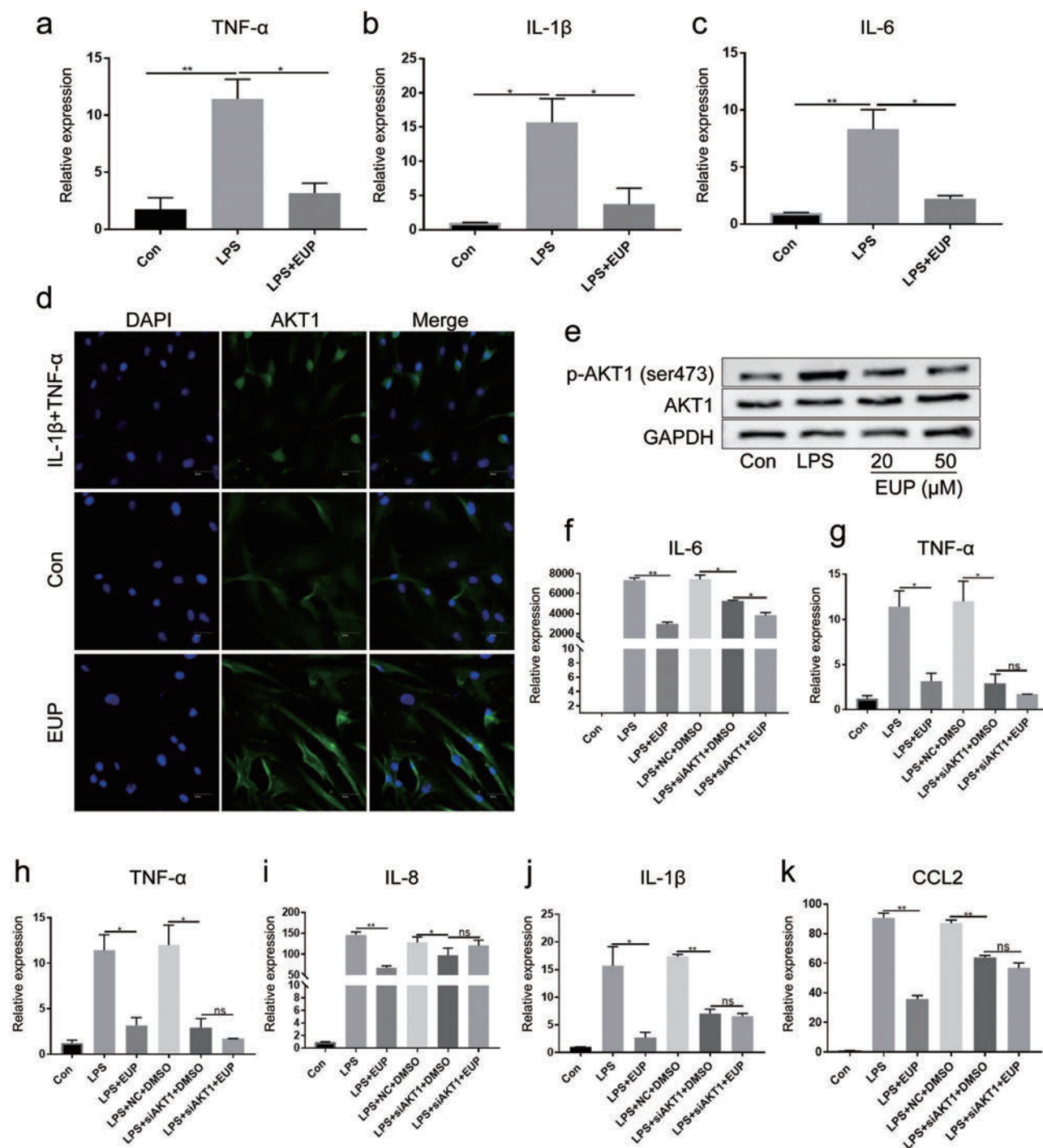


Fig. 5. EUP exerts anti-arthritis effects through the toll-like receptor signaling pathway. (a–c) After exposure to LPS, the levels of IL1 β , TNF- α and IL6 were determined by RT-qPCR. (d) The intracellular expression of AKT1 was detected by IF. (e) The western blot results revealed the protein levels of p-Akt (Ser473), Akt and GAPDH in RA FLSs treated with 20 μ M and 50 μ M of EUP. (f–k) The levels of IL6, IL1 β , TNF- α , IL8, MMP3 and CCL2 were detected by RT-qPCR. All data are representative of three independent experiments. The results were analyzed by one-way ANOVA, followed by Tukey's honest significant difference test. ns: non-significant, * $p < 0.05$, ** $p < 0.01$, vs. the indicated control group.

treatment options for patients, the development of new drugs is urgently needed.^{19,20}

There are a variety of TCMs in China. For example, astragaloside IV (AS-IV) is a cycloartane-type chemical and steroidal

glycoside, which exhibits pharmacological effects on anti-cancer and anti-inflammatory, has roles in the enhancement of resistance of the immune system, and attenuates the ability of migration and invasion of cancer cells. Its function is similar to EUP. The phar-

macological effects of AS-IV are associated with the inactivation of multiple signaling pathways, such as the RAF-MEK-ERK pathway and PI3K/Akt/NF- κ B pathway.²¹ Similarly, resveratrol regulates immunity by interfering with immune cell regulation, proinflammatory cytokine synthesis, and the gene expression.²² EUP is well-known for its biological activities. In the present study, it was found that EUP decreased the secretion of inflammatory factors to slow down the occurrence and development of RA. Data has shown that several phytochemicals with terpenic or phenolic structures are isolated from *Euphorbia lathyris*. EUP is isolated from *Euphorbia lathyris*, and has multidrug resistance (MDR)-reversing activity.²³ Recent studies have shown that EUP can inhibit adipogenesis in 3T3-L1 cells by activating the AMPK pathway.⁷ EUP has also been used as a TCM to treat cancer. In the present study, it was found that EUP treatment can ameliorate the arthritis phenotype of RA FLSs. More importantly, EUP treatment can suppress the severity of RA in CIA models. Thus, these present results suggest that EUP has potential in the treatment of RA.

In recent studies, network pharmacology has been applied to predict the targets of various drugs. This ended the traditional model of drug development dominated by “one drug, one target, one disease,” and introduced a new model of research on the complex network relationships between multiple targets and multiple diseases.^{24,25} In order to explore the molecular mechanism of EUP in the treatment of RA, network pharmacology was used to analyze the possible targets. Through network pharmacology, the KEGG pathway analysis of different expression levels of genes indicated that these genes are enriched in the pathway of osteoclast differentiation, apoptosis, the toll-like receptor signaling pathway, and folate biosynthesis. Importantly, the toll-like receptor signaling pathway has been proven to be associated with the development of RA.^{26,27} In the present study, STRING analysis and molecular docking were utilized, and it was predicted that AKT1, the key component in the toll-like receptor signaling pathway, is a potential target of EUP. AKT1 is ubiquitously expressed at high levels, suggesting the role of AKT1 in regulating cell function. After activation, AKT1 enters the nucleus and regulates a variety of cell activities, including cell proliferation and apoptosis, and its activity depends on the experimental condition.²⁸ Furthermore, AKT1 is also a crucial molecule in activating the NF- κ B signaling pathway.²⁹ All NF- κ B and Akt pathways are also involved in the anti-proliferative and anti-inflammatory effects of pitavastatin.³⁰ In the present study, the data revealed that EUP inactivates the toll-like receptor signaling pathway by inhibiting the nuclear translocation of AKT1 and its downstream effectors, further confirming the anti-arthritis role of EUP in RA.

Future directions

EUP is one of the major components of TCM, which has antiviral, antitumor, and other biological activities. The present study identified the novel role of EUP in RA treatment from a series of phenotypic and animal experiments. The detailed analysis also revealed that AKT1 serves as the potential target of EUP in RA, which provides a theoretical and experimental basis for EUP application in RA treatment. However, this still needs to be proven through clinical trials. The target of EUP was identified through network pharmacology and molecular docking technology, further confirming the importance of network pharmacology in target searching, and providing a theoretical basis for its application.

Conclusions

EUP can ameliorate the inflammatory phenotype of RA FLSs, and delay inflammatory progression and joint destruction in the CIA model. Furthermore, it was identified that EUP exerts its anti-RA effects through the toll-like receptor signaling pathway and its key component, AKT1, which was taken as a potential target. The present study revealed that EUP may be effective in RA treatment, although further studies are needed to clarify its potential for clinical tests.

Supporting information

Supplementary material for this article is available at <https://doi.org/10.14218/ERHM.2021.00076>.

Supplementary File 1. ARRIVE guidelines.

Acknowledgments

None.

Funding

This research was funded by the National Natural Science Foundation of China (Grant nos. 81772760 and 81901666), and the Taishan Scholar Project of Shandong Province (No. tsqn20161076).

Conflict of interest

The authors have no conflicts of interest related to this publication.

Author contributions

Study concept and design (GS); Conduction and performance of the study (HF, RZ, LS and SH); Collection of samples (LY, GY, ZY, SD and WT); Analysis and interpretation of data (LX, ZT, PJ and GL). All authors have made a significant contribution to the study, and approved the final manuscript.

Ethical statement

All 10 patients met the 1987 American College of Rheumatology revised RA diagnostic criteria, and all patients were informed and agreed to participate in the study. The present study conformed to the ethics guidelines of the Declaration of Helsinki. All appropriate measures were taken to minimize the pain or discomfort of animals. This study was carried out in accordance with the recommendations in the Guide for the Care and Use of Laboratory Animals of the Institutional Animal Care and Use Committee of Shandong First Medical University & Shandong Academy of Medical Sciences. The study protocol was approved by the Institutional Review Board of Shandong Medicinal Bio-technology Center (VCMC08BR067).

Data sharing statement

No additional data are available.

References

- [1] Sparks JA. Rheumatoid Arthritis. *Ann Intern Med* 2019;170(1):ITC1–ITC16. doi:10.7326/AITC201901010, PMID:30596879.
- [2] Wang L, Wang N, Zhao Q, Zhang B, Ding Y. Pectolinarin inhibits proliferation, induces apoptosis, and suppresses inflammation in rheumatoid arthritis fibroblast-like synoviocytes by inactivating the phosphatidylinositol 3 kinase/protein kinase B pathway. *J Cell Biochem* 2019;120(9):15202–15210. doi:10.1002/jcb.28784, PMID:31020684.
- [3] Abbasi M, Mousavi MJ, Jamalzehi S, Alimohammadi R, Bezvan MH, Mohammadi H, *et al.* Strategies toward rheumatoid arthritis therapy; the old and the new. *J Cell Physiol* 2019;234(7):10018–10031. doi:10.1002/jcp.27860, PMID:30536757.
- [4] Liu W, Zhang Y, Zhu W, Ma C, Ruan J, Long H, *et al.* Sinomenine Inhibits the Progression of Rheumatoid Arthritis by Regulating the Secretion of Inflammatory Cytokines and Monocyte/Macrophage Subsets. *Front Immunol* 2018;9:2228. doi:10.3389/fimmu.2018.02228, PMID:30319663.
- [5] Shi J, Chen Q, Xu M, Xia Q, Zheng T, Teng J, *et al.* Recent updates and future perspectives about amygdalin as a potential anticancer agent: A review. *Cancer Med* 2019;8(6):3004–3011. doi:10.1002/cam4.2197, PMID:31066207.
- [6] Lee WY, Chen HY, Chen KC, Chen CY. Treatment of rheumatoid arthritis with traditional chinese medicine. *Biomed Res Int* 2014;2014:528018. doi:10.1155/2014/528018, PMID:24991562.
- [7] Park SJ, Park JH, Han A, Davaatseren M, Kim HJ, Kim MS, *et al.* Euphorbiasteroid, a component of Euphorbia lathyris L., inhibits adipogenesis of 3T3-L1 cells via activation of AMP-activated protein kinase. *Cell Biochem Funct* 2015;33(4):220–225. doi:10.1002/cbf.3107, PMID:25914364.
- [8] Ren Q, Zhao S, Ren C, Ma Z. Astragalus polysaccharide alleviates LPS-induced inflammation injury by regulating miR-127 in H9c2 cardiomyoblasts. *Int J Immunopathol Pharmacol* 2018;32:2058738418759180. doi:10.1177/2058738418759180, PMID:29451405.
- [9] Ma JD, Jing J, Wang JW, Yan T, Li QH, Mo YQ, *et al.* A novel function of artesunate on inhibiting migration and invasion of fibroblast-like synoviocytes from rheumatoid arthritis patients. *Arthritis Res Ther* 2019;21(1):153. doi:10.1186/s13075-019-1935-6, PMID:31234900.
- [10] Song G, Feng T, Zhao R, Lu Q, Diao Y, Guo Q, *et al.* CD109 regulates the inflammatory response and is required for the pathogenesis of rheumatoid arthritis. *Ann Rheum Dis* 2019;78(12):1632–1641. doi:10.1136/annrheumdis-2019-215473, PMID:31455659.
- [11] Miyoshi M, Liu S. Collagen-Induced Arthritis Models. *Methods Mol Biol* 2018;1868:3–7. doi:10.1007/978-1-4939-8802-0_1, PMID:30244448.
- [12] Wang Q, Zhou X, Zhao Y, Xiao J, Lu Y, Shi Q, *et al.* Polyphyllin I Ameliorates Collagen-Induced Arthritis by Suppressing the Inflammation Response in Macrophages Through the NF- κ B Pathway. *Front Immunol* 2018;9:2091. doi:10.3389/fimmu.2018.02091, PMID:30319603.
- [13] Ishii S, Isozaki T, Furuya H, Takeuchi H, Tsubokura Y, Inagaki K, *et al.* ADAM-17 is expressed on rheumatoid arthritis fibroblast-like synoviocytes and regulates proinflammatory mediator expression and monocyte adhesion. *Arthritis Res Ther* 2018;20(1):159. doi:10.1186/s13075-018-1657-1, PMID:30071898.
- [14] Wei M, Li H, Li Q, Qiao Y, Ma Q, Xie R, *et al.* Based on Network Pharmacology to Explore the Molecular Targets and Mechanisms of Gegen Qinlian Decoction for the Treatment of Ulcerative Colitis. *Biomed Res* 2019;2019:192018. doi:10.1155/2019/192018, PMID:31000000.
- [15] Nygaard G, Firestein GS. Restoring synovial homeostasis in rheumatoid arthritis by targeting fibroblast-like synoviocytes. *Nat Rev Rheumatol* 2020;16(6):316–333. doi:10.1038/s41584-020-0413-5, PMID:32393826.
- [16] Smolen JS, Aletaha D, McInnes IB. Rheumatoid arthritis. *The Lancet* 2016;388(10055):2023–2038. doi:10.1016/S0140-6736(16)30173-8.
- [17] Küçükdeveci AA. Nonpharmacological treatment in established rheumatoid arthritis. *Best Pract Res Clin Rheumatol* 2019;33(5):101482. doi:10.1016/j.berh.2019.101482, PMID:31987686.
- [18] Wu Y, Zhang F, Yang K, Fang S, Bu D, Li H, *et al.* SymMap: an integrative database of traditional Chinese medicine enhanced by symptom mapping. *Nucleic Acids Res* 2019;47(D1):D1110–D1117. doi:10.1093/nar/gky1021, PMID:30380087.
- [19] Zhang J, Wu C, Gao L, Du G, Qin X. Astragaloside IV derived from Astragalus membranaceus: A research review on the pharmacological effects. *Adv Pharmacol* 2020;87:89–112. doi:10.1016/bs.apha.2019.08.002, PMID:32089240.
- [20] Malaguarnera L. Influence of Resveratrol on the Immune Response. *Nutrients* 2019;11(5):946. doi:10.3390/nu11050946, PMID:31035454.
- [21] Choi JS, Kang NS, Min YK, Kim SH. Euphorbiasteroid reverses P-glycoprotein-mediated multi-drug resistance in human sarcoma cell line MES-SA/Dx5. *Phytother Res* 2010;24(7):1042–1046. doi:10.1002/ptr.3073, PMID:19960428.
- [22] Li S, Zhang B. Traditional Chinese medicine network pharmacology: theory, methodology and application. *Chin J Nat Med* 2013;11(2):110–120. doi:10.1016/S1875-5364(13)60037-0, PMID:23787177.
- [23] Hopkins AL. Network pharmacology: the next paradigm in drug discovery. *Nat Chem Biol* 2008;4(11):682–690. doi:10.1038/nchembio.118, PMID:18936753.
- [24] Zenke K, Muroi M, Tanamoto KI. AKT1 distinctively suppresses MyD88-dependent and TRIF-dependent Toll-like receptor signaling in a kinase activity-independent manner. *Cell Signal* 2018;43:32–39. doi:10.1016/j.cellsig.2017.12.002, PMID:29242168.
- [25] Yu M, Zeng M, Pan Z, Wu F, Guo L, He G. Discovery of novel akt1 inhibitor induces autophagy associated death in hepatocellular carcinoma cells. *Eur J Med Chem* 2020;189:112076. doi:10.1016/j.ejmech.2020.112076, PMID:32007668.
- [26] Dai Q, Zhou D, Xu L, Song X. Curcumin alleviates rheumatoid arthritis-induced inflammation and synovial hyperplasia by targeting mTOR pathway in rats. *Drug Des Devel Ther* 2018;12:4095–4105. doi:10.2147/DDDT.S175763, PMID:30584274.
- [27] Zhu X, Song Y, Huo R, Zhang J, Sun S, He Y, *et al.* Cyr61 participates in the pathogenesis of rheumatoid arthritis by promoting prol-1 β production by fibroblast-like synoviocytes through an AKT-dependent NF- κ B signaling pathway. *Clin Immunol* 2015;157(2):187–197. doi:10.1016/j.clim.2015.02.010, PMID:25728492.
- [28] Chen Y, Wang Y, Liu M, Zhou B, Yang G. Diosmetin exhibits anti-proliferative and anti-inflammatory effects on TNF- α -stimulated human rheumatoid arthritis fibroblast-like synoviocytes through regulating the Akt and NF- κ B signaling pathways. *Phytother Res* 2020;34(6):1310–1319. doi:10.1002/ptr.6596, PMID:31833613.